

Effect of Ag₂O on cell viability of ZnO nanoparticle synthesized by low temperature solution synthesis process

Atanu Naskar^{1,*}, Batakrishna Jana², Hong Gun Kim¹, Lee Ku Kwac^{1,*}

¹Institute of Carbon Technology, Jeonju University 303 Cheonjam-ro, Wansan Gu, Jeonju, South Korea

²Department of Chemistry, Ulsan National Institute of Science and Technology (UNIST), 50 UNIST-gil, Eonyang-eup, Ulju-gun, South Korea

*corresponding author e-mail address: atanunaskar22@gmail.com, kwac29@jj.ac.kr

ABSTRACT

The synthesis, characterization and biomedical applications of mixed metal oxide is receiving increasing interest due to their property related specific applications. In this regard, ZnO and Ag₂O have been applied for different biomedical applications individually but the effect of Ag₂O on cell viability of ZnO has not been reported yet. The objective of this study is to see the effect of Ag₂O nanoparticle on cell viability of ZnO nanoparticles synthesized by adopting a two-step low temperature solution process. X-ray diffraction study confirms the co-existence of ZnO and Ag₂O phases. Transmittance electron microscopy has been used to characterize the morphological properties of the samples. X-ray photoelectron spectroscopic analysis also confirms the formation of ZnO-Ag₂O nanocomposite. The *in vitro* cytotoxicity with the help of MTT assay (upto a maximum of 200 µg/mL) on HeLa cell line approves that the ZnO-Ag₂O (ZSO) nanocomposite is more biocompatible than the individual ZnO and Ag₂O nanoparticle. This nanocomposite ZSO can be used as a vehicle for drug delivery systems.

Keywords: Low temperature solution process, ZnO, Ag₂O, mixed metal oxide nanocomposite, cell viability, Nanobiomaterial.

1. INTRODUCTION

Nanocomposites with mixed oxides have received growing interest due to their various applications in different biomedical applications like drug delivery, bioimaging, biosensing, antibacterial activity etc. [1]. The basic advantage of the mixed oxide is that the properties of the individual oxides can be tuned for a better functional nanocomposite whose activity would be much more effective than individual oxide. Most mixed oxides show the combined property of the individual oxides due to their interaction between constituent materials. Mixed metal oxide such as Fe₃O₄-Ag₂O [2], CuO-ZnO [3], CuO-NiO [4], Fe₃O₄-ZnO [5] has already been reported for different biomedical applications due to their showing of combined properties.

In recent years, nanosized ZnO and Ag₂O have been extensively used for numerous biomedical applications like antibacterial activity, anticancer activity, bioimaging, drug delivery etc. due to their unique physical and chemical properties [1, 6-7]. Therefore, it is not hard to detect the numerous reports on the biocompatibility of ZnO nanoparticle before its use for *in vivo* applications in cell systems regarding drug delivery and bioimaging studies. Ag₂O is a p-type semiconductor and has

mainly been used for antibacterial, anti-parasitic and photocatalytic activity [2]. Despite their advantageous properties regarding biomedical applications, no other study has shown the effect of Ag₂O on ZnO nanoparticle regarding biocompatibility. Therefore, developing a new mixed metal oxide nanocomposite combining ZnO and Ag₂O can give a new direction for different biomedical applications. In this respect, Fakhri et al. [2] showed that Fe₃O₄-Ag₂O quantum dots decorated cellulose nanofibers which can be used as a carrier of anticancer drugs for skin cancer. But, to the best of our knowledge, no other study has shown the cytotoxicity nature of ZnO-Ag₂O nanocomposite.

Therefore, in this present work, the effect of Ag₂O on cell viability of ZnO nanoparticle synthesized by low temperature solution synthesis has been explored. Two-step synthesis processes have been used to synthesize ZnO-Ag₂O nanocomposite. Then the synthesized samples were used for materials characterizations and systematic cell viability study on HeLa cell line. The cell viability result of the ZnO-Ag₂O nanocomposite showed admirable biocompatibility even in higher concentration which can be useful as a drug delivery vehicle for future applications.

2. MATERIALS AND METHODS

2.1. Synthesis of ZnO nanoparticles (ZO).

ZnO nanoparticles (ZO) were synthesized by a facile low temperature solution synthesis process. Initially, 50 mmol zinc chloride [(ZnCl₂, Junsei Chemical Co. Ltd ≥ 98%)] solution was prepared in 200 mL of deionized water. Then, NH₄OH (Junsei Chemical Co. Ltd, 28-30%) was added under continuous stirring to the zinc chloride solution until the pH of the medium reached to 10. After that, the solution was kept stirring at a constant temperature for 3h at 90°C. Then, the solid materials were

washed with deionized water and ethanol by centrifugation process for 3 – 4 times. Finally, the samples were dried in an air oven at ~60°C for 24 h duration.

2.2. Synthesis of ZnO-Ag₂O (ZSO) nanocomposite.

The synthesis of ZSO nanocomposite was made by using synthesized ZO nanoparticles, AgNO₃ (Junsei Chemical Co. Ltd), PEG-8000 (Sigma Aldrich) and NaOH. Initially, 0.4 g ZO nanoparticles and 2 g of PEG-8000 were uniformly dispersed in 100 mL of deionized water through a continuous stirring. Then 1.8

g of AgNO_3 was added to the mixture and stirred continuously for 30 minutes. After that, 0.2 M NaOH solution was added into the mixture dropwise for pH to reach 14 with continuous stirring. Next, the precipitate was separated out by centrifugation and product, ZSO was initially washed with deionized water followed by ethanol for 3-4 times. Finally, the product was dried in an air oven at $\sim 60^\circ\text{C}$ for 24 h. The similar process was followed for the synthesis of Ag_2O (SO) nanoparticles [8] without the addition of ZO nanoparticles.

2.3. Materials properties.

X-ray diffractometer (Philips PW3050 X-ray diffraction unit) with nickel filtered CuK_α radiation source ($\lambda = 1.54060 \text{ \AA}$) was used to obtain the X-ray diffraction (XRD) patterns of the samples (2 θ range, $5^\circ - 80^\circ$). Transmission electron-/high resolution transmission electron microscopy (TEM/HRTEM) measurements were performed by JEOL make (JEM-2010, Japan) instrument at an accelerating voltage of 200 kV. Carbon coated Cu grids were used for sample placement in this measurement. The samples were carefully placed onto separate Cu-grids after the dispersion in methanol by ultrasonication. X-ray photoelectron spectrum (XPS) with binding energy range, 200 – 1200 eV for ZSO was recorded to decide the chemical state of elements and chemical interaction/complexation of rGO with the inorganic moiety present in the sample by employing Theta Probe (Thermo Fisher Scientific Inc., USA) XPS microprobe surface analysis system.

3. RESULTS

3.1. Materials properties of nanocomposites.

3.1.1. Phase structure. X-ray diffraction study (Fig. 1) was used to check the crystallinity and crystal phases of as-synthesized ZnO (ZO), Ag_2O (SO) and ZnO- Ag_2O (ZSO) samples. It can be seen from the Figure 1, all the XRD peaks of ZO fully matched with hexagonal ZnO (h-ZnO) [JCPDS 36-1451] [1]. The diffraction peaks of SO nanoparticles were also matched well with the cubic structure of pure Ag_2O [JCPDS card no. 76-1393] [8]. There was no additional peak detected for SO nanoparticles confirming the purity of Ag_2O nanoparticles. Meanwhile, for ZSO nanocomposite, a mixed crystal phase (ZnO and Ag_2O) is observed from the XRD pattern of the sample which confirms that ZnO and Ag_2O coexist in the ZSO nanocomposite.

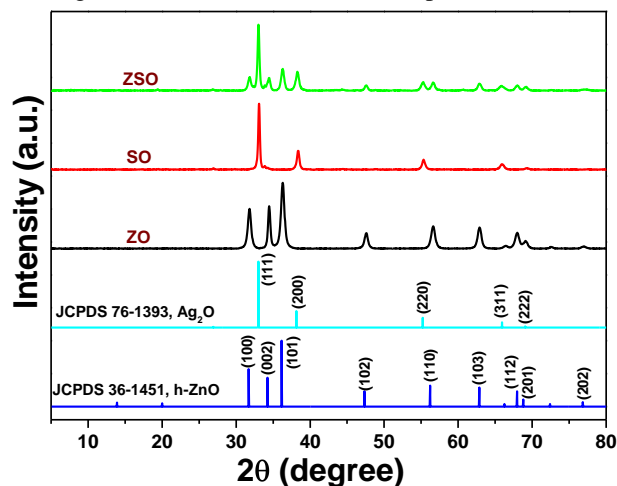


Figure 1. XRD patterns of ZO, SO and ZSO samples.

2.4. Cytotoxicity study.

The cytotoxicity of ZO, SO and ZSO samples was measured using HeLa cell line procured from ATCC, USA. Dulbecco's modified eagles medium (DMEM, Gibco, USA), fetal bovine serum (FBS, Gibco, USA), PenStrep (Gibco, USA) and MTT (3-[4,5-dimethylthiazol-2-yl]-2,5-diphenyltetrazoliumbromide, Sigma, USA) were used as essential chemicals and reagents for the study.

2.4.1. Measurement of in vitro cellular cytotoxicity by MTT assay.

HeLa cell line was cultured in DMEM (Gibco) supplemented with 10% fetal bovine serum (FBS) and antibiotic (1% penicillin/streptomycin) in 5% CO_2 at 37°C . MTT assay was used to measure the cellular toxicity. Initially, HeLa cells (10^4 cells per well) were seeded on to a flat bottom 96-well plate and incubated at 37°C in 5% CO_2 one day before the treatment. Then the cells were treated with or without (i.e. vehicle control) nanocomposite at different concentrations, ranging from 0 to 200 $\mu\text{g}/\text{mL}$ and kept for 24 h. Later, it was subjected to MTT assay. 100 μL of DMEM solution containing 10 μL of MTT (5 mg/mL) was added to each well. After 4 h of incubation, the media was removed and cells were dispersed in 100 μL of 1:1 (v/v) solvent mixture of dimethyl sulphoxide (DMSO) and Methanol. Absorbance spectra of the samples were measured at 570 nm wavelength by SpectraMax M5e Multi-Mode Microplate Reader. The cell viability values were expressed in percentages with respect to control values.

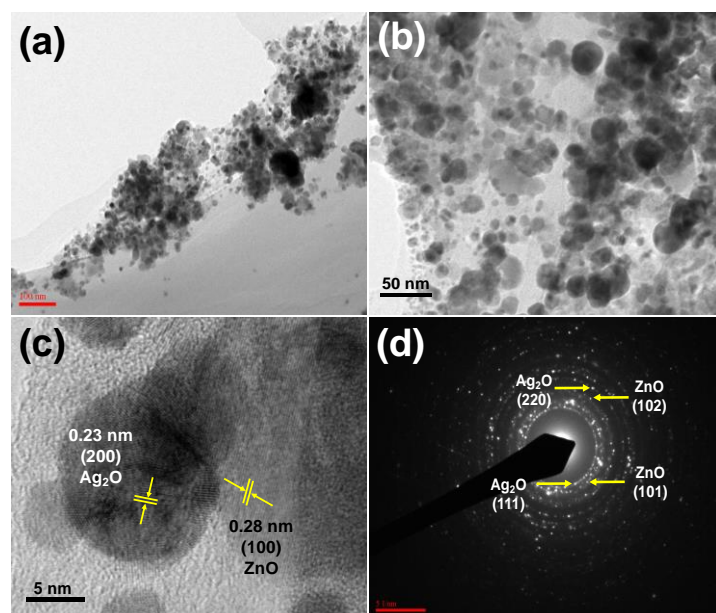


Figure 2. TEM images (a, b) of ZSO nanocomposite. HRTEM and SAED images of ZSO nanocomposite are shown in (c) and (d) respectively.

3.1.2 TEM microstructure. The TEM microstructure of the representative sample ZSO is shown in Figure 2a, 2b. The corresponding HRTEM of the sample is also shown in Figure 2c. It is evident from Figure 2c that distinct lattice fringes with an interplanar spacing of 0.28 nm can be found which can be indexed to (100) crystal plane of ZnO (ZO) [7]. Moreover, another lattice fringes with an interplanar spacing of 0.23 nm can also be found which corresponds to (200) crystal plane of Ag_2O [9]. Therefore,

the coexistence of ZnO and Ag₂O crystal phase structure of the ZSO sample can be confirmed the TEM result and fully corroborated with the XRD (Fig. 1) of the sample. Furthermore, Figure 2d shows the selected area electron diffraction (SAED) pattern of ZSO sample to confirm the coexistence of ZnO and Ag₂O crystal phase. The (101), (102) crystal planes of ZnO and (111), (220) crystal planes of Ag₂O can be clearly distinguishable from the rings present in Figure 2d. The TEM microstructure of ZSO sample confirms the formation of nanocomposite with ZnO and Ag₂O nanoparticle.

3.1.3 XPS analysis. Figure 3 shows the XPS data of the representative sample ZSO to understand the surface chemical composition and the valence state of the elements. The binding energy signals of Zn2p and Ag3d are shown in Figure 3a and 3b, respectively. As can be seen from the Figure 3a, two peaks at ~1022.1 eV and ~1045.2 eV can be seen for the binding energy signals of Zn 2p which can be assigned to the binding energy of Zn 2p_{3/2} and Zn 2p_{1/2}, respectively [6, 10]. The energy difference between Zn 2p_{3/2} and Zn 2p_{1/2} binding energy levels is ~ 23.1 eV. The energy difference level is also the confirmation of the oxidation state of Zn ions which is II [6, 11]. Moreover, the existence of Ag3d is also assessed and shown in Figure 3b. The peaks are found at ~367.4 eV and ~373.4 eV (Fig. 3b) can be assigned to Ag3d_{5/2} and Ag3d_{3/2}, respectively and also the characteristic peaks of Ag⁺ for Ag₂O in ZSO nanocomposite [8, 12]. Therefore, the XPS result is well supported the XRD data and confirmed the formation of ZnO-Ag₂O (ZSO) nanocomposite.

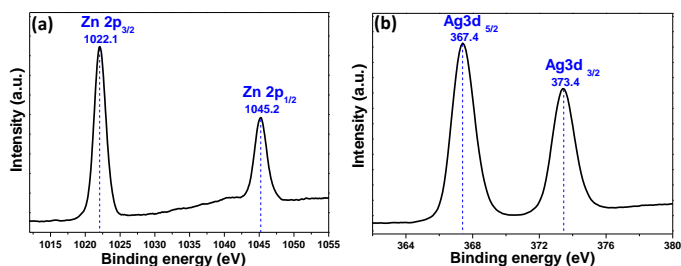


Figure 3. XPS data of ZSO sample: Binding energy spectrum of (a) Zn 2p and (b) Ag 3d core levels.

4. CONCLUSIONS

In conclusion, we can say that the zinc oxide (ZnO) - silver oxide (Ag₂O) nanocomposite (ZSO) has been successfully synthesized by adopting two-step low temperature solution process. X-ray diffraction study, transmittance electron microscopy and X-ray photoelectron spectroscopic analysis were

5. REFERENCE

- Naskar, A.; Khan, H.; Sarkar, R.; Kumar, S.; Halder, D.; Jana, S. Anti-biofilm activity and food packaging application of room temperature solution process based polyethylene glycol capped Ag-ZnO-graphene nanocomposite. *Mater. Sci. Eng. C* **2018**, *91*, 743–753, <https://doi.org/10.1016/j.msec.2018.06.009>.
- Fakhri, A.; Tahami, S.; Nejad, P.A. Preparation and characterization of Fe₃O₄-Ag₂O quantum dots decorated cellulose nanofibers as a carrier of anticancer drugs for skin cancer. *J Photochem. Photobiol. B* **2017**, *175*, 83–88, <https://doi.org/10.1016/j.jphotobiol.2017.08.032>.
- Saravanakkumar, D.; Sivaranjani, S.; Kaviyarasu, K.; Ayeshamariam, A.; Ravikumar, B.; Pandiarajan, S.; Veeralakshmi, C.; Jayachandran, M.; Maaza, M. Synthesis and characterization of ZnO-CuO nanocomposites powder by

3.2 In vitro cellular cytotoxicity .

MTT assay was performed on HeLa (Fig. 4) cell line for ZO, SO and ZSO samples to evaluate the cell viability effect of Ag₂O nanoparticle on ZnO nanoparticle by varying the concentration of samples. Each bar graph represents an average of three independent experiments. From Figure 4, it is clear that the ZSO nanocomposite is more biocompatible than individual metal oxides. Excellent cell viability of HeLa cells was observed for ZSO compared to ZO and SO samples with nearly ~70% of viable cells at 100 µg/ml dose with respect to the control. Therefore, it can be confirmed that although the SO is toxic to the HeLa cells, it is not affecting the biocompatibility of ZO nanoparticle. The nanocomposite can be used as a vehicle for drug delivery for future applications.

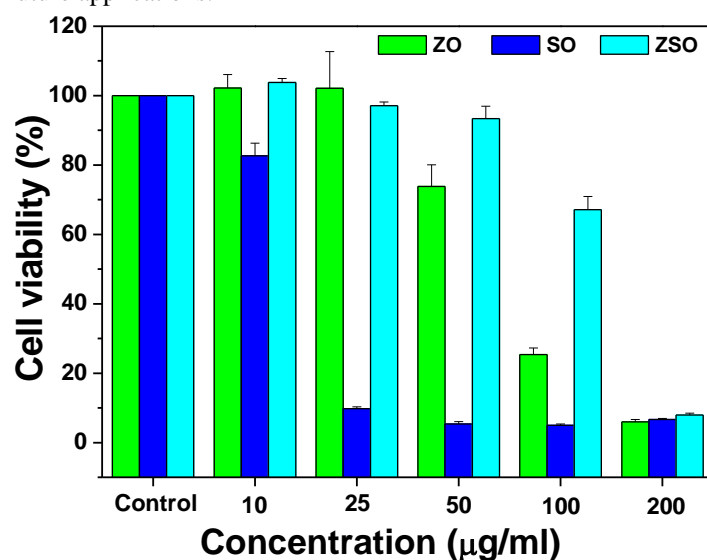


Figure 4. Cell viability from in vitro cellular cytotoxicity, MTT assay of HeLa cell line for ZO, SO and ZSO samples with varying concentrations. The error bars represent \pm SD ($P < 0.05$).

effectively used to confirm the formation of ZnO-Ag₂O nanocomposite. The MTT assay on HeLa cell line showed that the Ag₂O nanoparticle does not affect the biocompatibility of ZnO nanoparticles and can be used as a vehicle for drug delivery systems.

modified perfume spray pyrolysis method and its antimicrobial investigation. *J. Semicond.* **2018**, *39*, 033001.

4. Wang, Z.; Hai, J.; Li, T.; Ding, E.; He, J.; Wang, B. Pressure and fluorescence dual signal readout CuO-NiO/C heterojunction nanofibers-based nanoplatform for imaging and detection of target cancer cells in blood. *ACS Sustainable Chem. Eng.* **2018**, *6*, 9921–9929, <http://dx.doi.org/10.1021/acssuschemeng.8b01166>.

5. Madhubala, V.; Kalaivani, T. Phyto and hydrothermal synthesis of Fe₃O₄@ZnO core-shell nanoparticles using *Azadirachta indica* and its cytotoxicity studies. *Appl. Surf. Sci.* **2018**, *449*, 584–590, <https://doi.org/10.1016/j.apsusc.2017.12.105>.

6. Naskar, A.; Bera, S.; Bhattacharya, R.; Saha, P.; Roy, S.S.; Sen, T.; Jana, S. Synthesis, characterization and antibacterial activity of Ag incorporated ZnO-graphene nanocomposites. *RSC Adv.* **2016**, *6*, 88751–88761, <https://doi.org/10.1039/C6RA14808E>.
7. Naskar, A.; Bera, S.; Bhattacharya, R.; Roy, S.S.; Jana, S. Effect of bovine serum albumin immobilized Au-ZnO-graphene nanocomposite on human ovarian cancer cell. *J Alloys Compd.* **2018**, *734*, 66-74, <https://doi.org/10.1016/j.jallcom.2017.11.029>.
8. Xu, L.; Wei, B.; Liu, W.; Zhang, H.; Su, C.; Che, J. Flower-like ZnO-Ag₂O composites: precipitation synthesis and photocatalytic activity. *Nanoscale Res. Lett.* **2013**, *8*, 536, <https://doi.org/10.1186/1556-276X-8-536>.
9. Prakoso, S. P.; Taufik, A.; Saleh, R. One-step microwave-assisted colloidal synthesis of hybrid silver oxide/silver nanoparticles: characterization and catalytic study. *IOP Conf. Ser.: Mater. Sci. Eng.* **2017**, *188*, 012021, <https://doi.org/10.1088/1757-899X/188/1/012021>.
10. Khan, W.; Khan, F.; Ajmal, H.M.S.; Huda, N.U.; Kim, J.H.; Kim, S.D. Evolution of structural and optical properties of ZnO nanorods grown on vacuum annealed seed crystallites. *Nanomaterials (Basel)* **2018**, *8*(2), 68.
11. Zhang, Q.; Xu, M.; You, B.; Zhang, Q.; Yuan, H.; Ostrikov, K. Oxygen vacancy-mediated ZnO nanoparticle photocatalyst for degradation of methylene blue. *Appl. Sci.* **2018**, *8*, 353.
12. Akel, S.; Dillert, R.; Balayeva, N. O.; Boughaled, R.; Koch, J.; Azzouzi, M. E.; Bahnemann, D. W. Ag/Ag₂O as a Co-catalyst in TiO₂ photocatalysis: Effect of the co-catalyst/photocatalyst mass ratio. *Catalysts* **2018**, *8*, 647;

6. ACKNOWLEDGEMENTS

The authors thankfully acknowledge the support from Basic Science Research Program (2017R1D1A1B03028413) and (2016R1A6A1A03012069) through the National Research Foundation (NRF) funded by the Ministry of Education of Korea. We would also like to thank our colleagues for their enthusiasm and cooperation in the study.



© 2019 by the authors. This article is an open access article distributed under the terms and conditions of the Creative Commons Attribution (CC BY) license (<http://creativecommons.org/licenses/by/4.0/>).